Downloaded from ascelibrary.org by Indian Institute of Technology, Hyderabad on 11/11/22. Copyright ASCE. For personal use only; all rights reserved.

Modeling Operating Speed Using Continuous Speed Profiles on Two-Lane Rural Highways in India

Vinayak Malaghan[1]; Digvijay S. Pawar[2]; and Hussein Dia, F.ASCE[3]

Abstract: The geometric elements of the road, such as tangents and curves, play a vital role in road safety because significant crashes are reported on the horizontal curves and tangent-to-curve transitions. Literature reveals that inconsistent geometric design of roads violates driver's expectation of operating speed leading to crashes. For safe manoeuver, it is necessary to achieve consistent operating speed with road geometry based on the driver's expectations rather than the designer's perception. Estimation of reliable operating speeds in the design phase will help to design safer road alignments. Several past studies developed operating speed models on the curves and tangent-to-curve transitions. However, these models used spot speed data with the assumption that the constant speed persists on the horizontal curves and entire deceleration/acceleration occurs on the approach/departure tangents. In this study, an instrumented vehicle with a high-end GPS (global positioning system) device was used to obtain the continuous speed profiles for passenger cars which resulted in reliable and robust speed prediction models for a tangent, curve, and tangent-to-curve. The study also establishes a relationship between the differential of the 85th percentile speed (ΔV_{85}) and 85th percentile speed differential ($\Delta_{85}V$). The analysis results revealed that ΔV_{85} underestimates $\Delta_{85}V$ by 5.32 km/h, and $\Delta_{85}V$ predicted the actual speed reduction from tangent-to-curve transitions. Statistical analysis results showed low errors, variations, and strong correlation of the proposed models with the field data. The models developed in the present study were validated and compared with various other models available in the literature. The comparative study highlights the importance of using continuous speed profile data to calibrate the operating speed models. **DOI: 10.1061/JTEPBS.0000447.** *© 2020 American Society of Civil Engineers.*

Author keywords: Geometric design consistency; Horizontal curves; Global positioning system (GPS); Design speed; Road geometry; Road safety.

Introduction

The three major factors which contribute to road crashes are driver, vehicle, and road infrastructure. Road infrastructure alone accounts for 34% of road crashes (Ahmed 2013). In India, road infrastructure accounted for a total of 467,044 crashes, among which 19,996 fatal crashes and 67,878 injury crashes were reported on horizontal curves (MORTH 2018). The percentage increase in crashes on horizontal curves was found to be 18.5% for the year 2018 compared with 2017. The crash statistics related to road infrastructure indicate that the geometric design consistency of the road elements (tangents and curves) plays a vital role in road crashes (García et al. 2013).

Highway geometric design consistency aims at coordinating the successive road geometric elements (tangent and curve) to ensure the geometric design conformance to driver's expectations to achieve harmonious travel along the roadway section (Gibreel et al. 1999). The geometric design consistency is assessed using measures like operating speed, side friction, vehicle dynamics, alignment indices, and mental workload (Gibreel et al. 1999; Hassan 2004). Among the various techniques, operating speed is the most commonly used measure to evaluate design consistency. Operating speed is the 85th percentile speed value at which drivers are observed to operate their vehicles during the free-flow condition (AASHTO 2011).

The design consistency based on the operating speed is evaluated using two approaches: (1) the difference between the operating speed and design speed value for individual geometric elements, and (2) the difference in the operating speed on the successive geometric elements. The geometric feature is considered to be inconsistent if the speed difference is higher than a certain threshold value. For example, Lamm et al. (1999) classified geometric elements as good (if $\Delta V_{85} < 10$ km/h), fair ($10 < \Delta V_{85} \leq 20$ km/h) and poor ($\Delta V_{85} > 20$ km/h) based on the difference in speed between successive geometric elements. Ottesen and Krammes (2000) found that the crash rates on curves increase with the increase in speed reduction from tangent-to-curve. The sudden change in the speed may surprise drivers and might lead to critical maneuvers resulting in a higher chance of collision (Krammes et al. 1997). More often, at higher speeds the vehicles are likely to leave the travel lane of the roadway while traversing the horizontal curves, thus leading to crashes (Albin et al. 2016). Therefore, the horizontal curves and tangent-to-curve transitions are more often identified as critical locations subjected to a lack of geometric design consistency. Several models, such as speed prediction models and deceleration/acceleration models, were developed as a function of various geometric variables to evaluate the design consistency (Misaghi and Hassan 2005; Jacob and Anjaneyulu 2013; Pérez-Zuriaga et al. 2013). The spot speed data collection method in these studies

[1]Research Scholar, Transportation Systems Engineering, Dept. of Civil Engineering, Indian Institute of Technology Hyderabad, Kandi, Medak 502285, India. Email: ce17resch11011@iith.ac.in

[2]Assistant Professor, Transportation Systems Engineering, Dept. of Civil Engineering, Indian Institute of Technology Hyderabad, Kandi, Medak 502285, India (corresponding author). Email: dspawar@iith.ac.in

[3]Professor, Dept. of Civil and Construction Engineering, Swinburne Univ. of Technology, Melbourne, VIC 3122, Australia. ORCID: https://orcid.org/0000-0001-8778-7296. Email: hdia@swin.edu.au

Note. This manuscript was submitted on January 11, 2020; approved on June 15, 2020; published online on August 19, 2020. Discussion period open until January 19, 2021; separate discussions must be submitted for individual papers. This paper is part of the ***Journal of Transportation Engineering, Part A: Systems***, © ASCE, ISSN 2473-2907.

allowed speed data to be collected at a specific location on the curve (usually midpoint of the curve) and tangent (Zuriaga et al. 2010). Thus, the models developed using single point speed measurements may not yield robust and reliable predictions (Zuriaga et al. 2010), and therefore, the transferability of the models is a concern. Hence, it is important to understand the continuous speed variation from tangent-to-curve and curve-to-tangent transitions to develop robust operating speed models on tangents, curves, and tangent-to-curve transitions.

In this study, vehicles fitted with a high-end GPS device were used to obtain continuous speed profiles. The paper aimed to understand the speed variation and develop speed prediction models on geometric elements such as tangents and curves. So far, no studies are reported in India which have developed the design consistency models using the instrumented vehicle to obtain continuous speed profiles for two-lane rural highways.

Literature Review

Operating speed is one of the various measures used for developing speed prediction models to evaluate highway geometric design consistency. The speed prediction models found in the literature are based on single element consistency (the difference between operating speed and design speed for individual geometric elements) and speed differential models for successive geometric elements.

Speed Prediction Models Based on Spot Speed Measurements

Several past studies used spot speed data to develop the operating speed models for selected geometric elements (tangent or curve). The spot data collection method allowed the operating speed data to be measured at a single point on tangent or curve. Thus, most of the proposed models assumed constant operating speed on curves, which indicates the entire speed variation occurs on the approach and the departure tangents (Ottesen and Krammes 2000; Fitzpatrick and Collins 2000; Lamm et al. 1988; Andueza 2000; Passetti and Fambro 1999; Al-Masaeid et al 1995; Maji et al. 2018; Misaghi and Hassan 2005; Jacob and Anjaneyulu 2013). Based on the above assumption, most of the previous studies collected spot speed data at the midpoint of the curve (MC) and at the specific locations on the approach/departure tangents to develop the speed prediction models (Montella et al. 2014; Ottesen and Krammes 2000).

Lamm et al. (1988) identified 11 spots on the approach tangent from the beginning of the curve to measure operating speed for the selected road stretch. The study assumed constant operating speed on horizontal curves, and the entire speed variation of the vehicle takes place on the approach and departure tangent. The study proposed an operating speed model for horizontal curves as a function of curvature change rate (CCR). The speed on the tangent was predicted from the same model assuming CCR as zero. The authors found that the operating speed at the beginning of the curve was 6.44–8.05 km/h higher than at the end of the curve. Ottesen and Krammes (2000) also developed an operating speed model for horizontal curves based on the same assumption made by Lamm et al. (1988). The spot speed measurements were taken for passenger cars at the approach tangent and midpoint of the curve. The speed on the tangent was set to 97.9 km/h by taking the mean of the observed speeds. The speed profile model developed was used to estimate the speed reduction from an approach tangent to horizontal curve. Similarly, Fitzpatrick and Collins (2000) studied the design consistency for rural highways based on the above-mentioned assumption. The operating speed on the long tangent was set to 100 km/h. Spot speed data were collected at the midpoint of the 21 horizontal curves. The authors developed speed prediction models for horizontal curves, vertical curves, and the combination of both using speed profiles. The models were used to evaluate design consistency based on the speed difference threshold values between geometric elements given by Lamm et al. (1999).

Previous studies considered simple horizontal curves in the development of speed prediction models. Passetti and Fambro (1999) studied the influence of circular curves with and without a spiral transition on the operating speed. The authors used traffic counters/classifiers and radar guns to measure the operating speeds of passenger cars at the MC and preceding tangent. The study concluded that for the range of data analyzed, circular curves with spiral transitions did not affect the operating speed of the passenger cars in comparison with simple circular curves. Another study by Gibreel et al. (2001) considered a horizontal curve combined with a vertical sag curve and a horizontal curve combined with a vertical crest curve for spiral transitions. The operating speed data were collected at five points, namely point of curvature (PC), point of tangency (PT), and mid curve (MC), and 60–80 m on the approach and departure tangent from the beginning and end of spiral curve, respectively. Operating speed models were developed at each of the five locations considering both horizontal and vertical alignment.

Past studies developed speed prediction models for plain and rolling terrain. Andueza (2000), on the other hand, developed the models for operating speed on tangent and curve for mountainous roads. Spot speed measurements were taken at the MC and tangent. The results of the study showed that speed and comfort are found to be the two efficiency measures drivers consider on horizontal curves. Therefore, drivers generally sacrifice one to the other as it is challenging to achieve higher speed with great comfort.

Some researchers, on the other hand, studied the influence of road geometry on operating speed of different vehicle types. Al-Masaeid et al. (1995) and Jacob and Anjaneyulu (2013) developed the operating speed prediction models for different vehicle classes using the trap line method for speed measurement. Studies concluded that class wise analysis of road geometric influence on operating speed of different vehicle types can enhance road safety.

Most of the speed prediction models were developed for two-lane rural highways. Sil et al. (2019) developed speed prediction models on horizontal curves for four-lane divided highways. The authors used video processed data to extract the speed of the vehicles at the midpoint of curve, point of curvature (PC), point of tangency (PT), and 50 m from the PC. The curve length, deflection angle, and preceding tangent length were found to be three significant parameters for the speed prediction models.

Speed Differential Models for Successive Geometric Elements Using Spot Speed and Continuous Speed Data

Al-Masaeid et al. (1995) developed differential of the 85th percentile operating speed (ΔV_{85}) models for different vehicle types (passenger cars, light trucks, and trucks) on two-lane rural highways. The study measured speeds at two locations on the curve and one location on the tangent. For each location and type of vehicle, the speed followed a normal distribution. The developed models were based on the hypothesis that the 85th percentile driver in the tangent speed distribution would be the 85th percentile driver in the curve speed distribution. However, Hirsh (1987) suggested theoretically that the driver corresponding to 85th percentile speed on the tangent may not remain the same for the 85th percentile speed on the curve. Therefore, 85th percentile speed differential $(\Delta_{85}V)$ for individual vehicles from tangent-to-curve transition was used to determine the actual speed reduction.

J. Transp. Eng., Part A: Systems, 2020, 146(11): 04020124

Downloaded from ascelibrary.org by Indian Institute of Technology, Hyderabad on 11/11/22. Copyright ASCE. For personal use only; all rights reserved.

Several studies developed $\Delta_{85}V$ models and established the relationship between $\Delta_{85}V$ and ΔV_{85}. Misaghi and Hassan (2005) and Castro et al. (2011) used the spot speed device to measure the speed at the approach tangent and midpoint of the curve. The authors developed the relation between $\Delta_{85}V$ and ΔV_{85} and concluded that ΔV_{85} underestimated $\Delta_{85}V$ by 7.55 and 4.49 km/h, in their respective studies. In the study by Jacob and Anjaneyulu (2013), ΔV_{85} underestimated $\Delta_{85}V$ by 1.27 km/h for passenger cars and 1.29 km/h for the combined vehicle classes (two-wheeler, car, truck, and bus).

In the previous literature, two assumptions were made in developing the speed models: (1) speed remains constant on the horizontal curves, and the entire speed variation takes place on approach/departure tangents, and (2) the driver corresponding to the 85th percentile speed on the tangent may remain the same for the 85th percentile speed on the curve. McFadden and Elefteriadou (2000) investigated the assumptions by increasing the number of speed measurement locations on the tangent and curve using spot speed measurement device. Authors compared the results of 85S2 (difference in 85th percentile operating speed at the midpoint of the tangent and 85th percentile operating speed at the midpoint of the curve considering two locations from tangent-to-curve), and 85S9 (difference in the maximum 85th percentile operating speed on the tangent and minimum 85th percentile operating speed on a curve considering nine locations from tangent-to-curve for entire driver population) with 85MSR (85th percentile maximum speed reduction from tangent-to-curve for individual driver or vehicle). The results showed that 85 MSR showed the actual maximum speed reduction in comparison with 85S2 and 85S9. The authors concluded that the location of maximum speed on the tangent would not occur at a specific location on the approach tangent, and the occurrence of the minimum operating speed on the curve might not coincide with the midpoint of the curve.

Later, the limitations due to spot speed data were overcome by using the driver simulator and GPS devices which facilitated to trace the continuous speed variation on tangent-to-curve transitions. The studies based on driver simulator inferred that ΔV_{85} underestimated $\Delta_{85}V$ by 2.32 km/h (Montella et al. 2014) and 1.66 km/h (Calvi and Bella 2014). Choudhari and Maji (2019) used the driver simulator and developed a multiple linear regression model to predict 85 MSR (85th percentile maximum speed reduction). The study developed a nomogram for safety evaluation of the horizontal curves for rural roads.

Research experiments based on a driving simulator to assess design consistency were further improved using the instrumented vehicle with a GPS device to obtain continuous speed profiles in a real-world environment. Pérez-Zuriaga et al. (2013) and Montella et al. (2014) used the instrumented vehicle to model the operating speed and found that ΔV_{85} underestimated $\Delta_{85}V$ by 5.31 and 6.16 km/h, respectively.

Recent studies in the US evaluated driver behavior on horizontal curves using NDS (Naturalistic Driving study) data conducted through the Strategic Highway Research Program (SHRP 2), which forms the largest dataset up to date (Dhahir and Hassan 2018). Dhahir and Hassan (2019) studied driver behavior on horizontal curves and tangents using NDS. The authors found that the speed difference at a specific location on the approach tangent and the midpoint of the curve was lower than the difference of maximum and minimum speed on the tangent and curve, respectively. The conclusions were in line with the conclusions driven by McFadden and Elefteriadou (2000).

Summarizing the literature, operating speed models were developed on the tangent and curve based on the single geometric element consistency approach. Further, the speed reduction models were developed for successive geometric elements, i.e., tangent-to-curve transitions. The studies found that the differential of the 85th percentile speed (ΔV_{85}) underestimated the actual speed reduction from tangent to curves. Hence, the 85th percentile speed differential $(\Delta_{85}V)$ approach was proposed to estimate the actual speed reduction from tangent-to-curve transitions. Although many models were developed to predict the operating speed on a tangent, curve, and tangent-to-curve transition, the reliability of the developed models is a concern (Hassan 2004).

In the present study, the operating speed variation from tangent-to-curve and the curve-to-tangent transition was studied. The study did not make any assumptions on the location of the maximum and minimum operating speed on the tangent and curve, respectively. The continuous speed profile allowed the identification of the actual maximum and minimum operating speed on the approach tangent and horizontal curve, respectively. Also, the reliability of the proposed models is validated with field data to check the prediction accuracy.

Objectives

The primary objectives of this paper are; (1) To develop the operating speed prediction models for different geometric elements (tangent and curve) as a function of various geometric variables such as preceding tangent length (P_{tl}), succeeding tangent length (S_{tl}), curve radius (R), curve length (L_c), deflection angle (Δ), and degree of curve (D_c) using continuous speed profile data; (2) To establish a relationship between the 85th percentile speed differential $(\Delta_{85}V)$ and the differential of the 85th percentile speed (ΔV_{85}); and (3) Validation and comparison of developed models with the existing speed models from different countries.

Data Collection

The continuous speed profiles were collected for different types of light motor vehicles such as hatchback, sedan, and sports utility vehicles. All these vehicles were clubbed under the single category *passenger car* for model development. The data collection was done during the day time in dry weather conditions. The vehicle was mounted with a GPS device, with the camera fixed to the windshield, the magnetic antenna on the roof of the car, and the GPS box placed near the dashboard [Fig. 1(a)].

Vehicle position, speed, distance, and deceleration/acceleration rate were recorded at every 0.1 s and stored in the internal data storage. The device was mounted and unmounted at the beginning and endpoint, respectively, of each trip by the research student. A driver questionnaire survey was conducted at the end of the trip, which included driver age, gender, and driving experience. A total of 49 drivers (ages between 21 and 59 years), with an average age of 33 years, voluntarily participated in the study. The driving experience varied from 1–38 years, with an average of 10 years.

During the data collection process, the drivers were informed about the purpose of fitting the GPS device in their vehicles. The drivers were instructed that the GPS device will be fitted to the windshield of the car, and the data will be collected for the institute's research project and not for any legal enforcement. No speed restrictions were imposed on the drivers. Also, the drivers were encouraged to drive as they usually do.

Six two-lane undivided rural roads in the states of Karnataka and Telangana, India, were selected for the study. Typical cross-section details of the selected road stretches are shown in Figs. 1(b and c). The data collection was limited to horizontal alignment in plain terrain with grade $< \pm 4\%$. In total, 49 horizontal

Downloaded from ascelibrary.org by Indian Institute of Technology, Hyderabad on 11/11/22. Copyright ASCE. For personal use only; all rights reserved.

Downloaded from ascelibrary.org by Indian Institute of Technology, Hyderabad on 11/11/22. Copyright ASCE. For personal use only; all rights reserved.

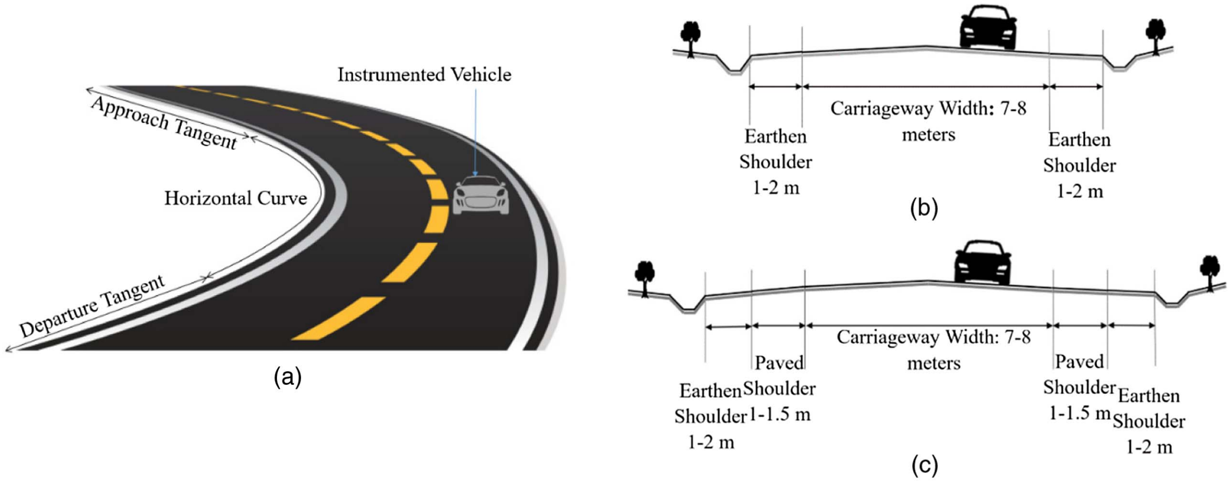

Fig. 1. (a) Schematic representation of geometric elements and the instrumented vehicle; (b) typical cross-section details of the selected sites MDR, SH17, SH 53, SH 135; and (c) NH 161.

Table 1. Summary of the road segments

Site	(1) MDR	(2) SH 17	(3) SH 17	(4) SH 53	(5) SH 53	(6) SH 135	(7) NH161
Road segment length (km)	3.2	23.94	22.84	4.44	8.26	15.9	3.38
Lane width (m)	3–3.125	3.5	3–3.5	3–3.25	3–3.25	2.75–3	3–3.5
Paved shoulder width (m)	NA	NA	NA	NA	NA	NA	1.5
Number of curves	4	4	9	14	3	11	4
Number of tangents	6	6	14	19	5	15	5
Independent tangents	5	6	14	13	4	15	4
Observations	54	70	70	87	87	91	48

Note: MDR = major district road; SH = state highway; and NH = national highway.

curves were selected with radii ranging from 60 to 800 m with an average radius of 266 m. The minimum and maximum curve lengths were 42 and 740 m, respectively, with an average of 165 m. The chosen curve sites were free from merging/diverging approaches, stop-controlled or signalized intersections, narrow bridge, and low traffic volume to ensure free-flow conditions. Independent tangents preceded each of the chosen 43 curves in both directions; however, six curves were found to be preceded by a dependent tangent in only one direction. A tangent was considered to be independent if its length exceeds 200 m (Dhahir and Hassan 2019; Fitzpatrick et al. 2000). The summary of the road segments and the number of observations per site are presented in Table 1.

Preliminary Analysis

Data Processing and Reduction

The data processing and reduction were carried out using highway design software (Civil 3D) and data analysis software (R Studio). The alignments of the road sections were designed in the design software in accordance with field conditions. The data samples were segmented into approach tangent, departure tangent, and curve portion referencing position coordinates. The segmented data consists of different parameters such as time, speed, acceleration/deceleration, distance, and position at every 0.1 s.

The next step after data processing involved eliminating the affected speed data segments or samples by observing speed profiles and video data. In total, 3,798 speed profiles were extracted which are reduced to 2,310 speed profiles after removing the affected data samples. The following criteria were considered to eliminate the affected data samples to study the effect of road geometry on driver operating speed choice:

1. The trajectory of each data sample generated was checked for abnormalities due to the signal loss. The data other than the signal issue were trimmed for further segmentation and analysis.
2. The curves characterized by speed humps at the point of curvature and point of tangency were excluded from the analysis.
3. The speed data affected in the approach tangent and curve portion due to the vehicle interaction (sudden entry at the curve/tangent, presence of lead vehicles) were discarded.
4. The speed profiles affected due to the pedestrian and animal crossing were also discarded from the analysis.

Correlation Test

Correlation between different geometric variables such as curve radius, curve length, deflection angle, tangent length, and 85th percentile operating speed on specific geometric elements were checked before developing the models. The variables showing significant correlation were further selected in the development of the regression models. The bivariate (Pearson) correlation matrix was used to describe the strength of the relationship between quantitative variables. Krehbiel (2004) introduced the following rule of thumb to decide if the observed value of the correlation coefficient is significant or not:

Table 2. Thresholds for the significance of the correlation between two variables

Sr. No	Geometric element	n	$2/\sqrt{n}$
1.	Curve	38	0.33
2.	Tangent	34	0.34
3.	Tangent-to-curve	35	0.34

Rule of Thumb: If $|r_{xy}| \geq 2/\sqrt{n}$, then a linear relationship exists.

where r_{xy} is the value of the correlation coefficient value between two variables x and y, and n is the number of observations.

The threshold values $(2/\sqrt{n})$ to check the correlation for different geometric elements, i.e., curve, tangent, and tangent-to-curve are shown in Table 2. The correlation between each of the variables was found to be rational and in the expected direction (Table 3). The values of the correlation coefficient greater than the threshold values and statistically significant at 95% confidence interval are shown in Table 3.

Model Development

All subset regression approach was used for developing operating speed models. This regression approach involves examining all the possible combinations of regression models from the independent variables. For example, if we have k regressors then the number of models that can be formed is two to the power of k (Wang and Chen 2016). All subset regression evaluates all the possible combinations of independent variables and presents the model with the best candidate variable (Elliott et al. 2013; Kabacoff 2011). The explanatory variables studied in the model development were curve radius (R), deflection angle (Δ), curve length (L_C), preceding tangent length (P_{tl}), succeeding tangent length (S_{tl}), and degree of curve (D_C). The following conditions were also checked while developing the regression models:

1. The coefficient of determination R^2 must be significant at the 95% confidence interval.
2. The coefficient of the independent variables used in the development of the models is significantly different from zero at the 95% confidence interval.
3. The direct or inverse relation of the explanatory variables with the response variable must have a rational interpretation.
4. The developed models were checked for the assumptions made in the OLS (ordinary least square) regression.

Operating Speed Model on Curve

The continuous speed profile data on the curves and the geometric design variables were used for developing operating speed models

Table 3. Bivariate (Pearson) correlation matrix

Coorelation of geometric elements	Variables	Pearson test	V_{85}	R	L_c	D_C	Δ	P_{tl}
Correlation for operating speed on the curves	R	Pearson(r)	0.84[a]	—	—	—	—	—
		Sig. (2-tailed)	0.00	—	—	—	—	—
	L_C	Pearson(r)	0.57[a]	0.74[a]	—	—	—	—
		Sig. (2-tailed)	0.00	0.00	—	—	—	—
	D_c	Pearson(r)	−0.92[a]	−0.79[a]	−0.61[a]	—	—	—
		Sig. (2-tailed)	0.00	0.00	0.00	—	—	—
	Δ	Pearson(r)	−0.35[a]	−0.16	0.41[a]	0.28	—	—
		Sig. (2-tailed)	0.03	0.33	0.01	0.09	—	—
	P_{tl}	Pearson(r)	0.61[a]	0.62[a]	0.43[a]	−0.55[a]	−0.07	—
		Sig. (2-tailed)	0.00	0.00	0.01	0.00	0.67	—
	S_{tl}	Pearson(r)	0.50[a]	0.35[a]	0.52[a]	−0.50[a]	0.19	0.34[a]
		Sig. (2-tailed)	0.00	0.03	0.00	0.00	0.26	0.04
Correlation for operating speed on tangents	R	Pearson(r)	0.42[a]	—	—	—	—	—
		Sig. (2-tailed)	0.01	—	—	—	—	—
	L_C	Pearson(r)	0.33	0.76[a]	—	—	—	—
		Sig. (2-tailed)	0.06	0.00	—	—	—	—
	D_c	Pearson(r)	−0.51[a]	−0.78[a]	−0.60[a]	—	—	—
		Sig. (2-tailed)	0.00	0.00	0.00	—	—	—
	Δ	Pearson(r)	−0.03	−0.15	0.17	0.14	—	—
		Sig. (2-tailed)	0.88	0.41	0.33	0.43	—	—
	P_{tl}	Pearson(r)	0.62[a]	0.66[a]	0.40[a]	−0.62[a]	−0.15	—
		Sig. (2-tailed)	0.00	0.00	0.02	0.00	0.39	—
	S_{tl}	Pearson(r)	0.51[a]	0.29	0.46[a]	−0.43[a]	0.18	0.40[a]
		Sig. (2-tailed)	0.00	0.10	0.01	0.01	0.31	0.02
Correlation for operating speed reduction from tangent-to-curve transitions	R	Pearson(r)	−0.78[a]	—	—	—	—	—
		Sig. (2-tailed)	0.00	—	—	—	—	—
	L_C	Pearson(r)	−0.54[a]	0.73[a]	—	—	—	—
		Sig. (2-tailed)	0.00	0.00	—	—	—	—
	D_c	Pearson(r)	0.86[a]	−0.75	−0.53[a]	—	—	—
		Sig. (2-tailed)	0.00	0.00	0.00	—	—	—
	Δ	Pearson(r)	0.40[a]	−0.33	0.23	0.51[a]	—	—
		Sig. (2-tailed)	0.02	0.05	0.17	0.00	—	—
	P_{tl}	Pearson(r)	−0.22	0.27	0.22	−0.15	−0.06	—
		Sig. (2-tailed)	0.21	0.11	0.21	0.39	0.74	—
	S_{tl}	Pearson(r)	0.34[a]	0.36[a]	0.32	−0.38[a]	−0.14	0.67[a]
		Sig. (2-tailed)	0.05	0.04	0.06	0.02	0.41	0.00

[a]Correlation is significant at 95% confidence interval.

Downloaded from ascelibrary.org by Indian Institute of Technology, Hyderabad on 11/11/22. Copyright ASCE. For personal use only; all rights reserved.

Table 4. Summary of the developed models

Model No.	Model	EV	VIF	SE	*t*-stat	*p*-value	R^2	AIC
	Operating speed models on curves							
1	$V_{85} = 11.68 + 10.37ln(R)$	R	—	0.67	15.38	0.00	0.87	197.35
2	$V_{85} = 84.72 - 10.37ln(D_C)$	D_C	—	0.67	−15.38	0.00	0.87	197.35
3	$V_{85} = 71.70 + 0.01R - 1.13D_C$	R	2.66	0.00	3.19	0.00	0.89	193.45
		D_C	2.66	0.15	−7.46	0.00	—	—
4	$V_{85} = 62.02 + 0.03R - 0.12\Delta$	R	1.03	0.00	9.47	0.00	0.75	222.99
		Δ	1.03	0.05	−2.58	0.01	—	—
5	$V_{85} = 72.91 + 0.05L_C - 0.37\Delta$	L_C	1.20	0.01	8.86	0.00	0.73	226.57
		Δ	1.20	0.05	−7.28	0.00	—	—
6	$V_{85} = 72.10 + 0.02R - 0.01L_C - 1.14D_C$	R	3.74	0.00	3.95	0.00	0.90	190.79
		L_C	2.25	0.01	−2.11	0.04	—	—
		D_C	2.67	0.14	−7.93	0.00	—	—
7	$V_{85} = 73.35 + 0.01R - 1.05D_C - 0.06\Delta$	R	2.68	0.00	3.52	0.00	0.90	190.88
		D_C	2.84	0.15	−7.03	0.00	—	—
		Δ	1.10	0.03	−2.09	0.04	—	—
8	$V_{85} = 69.87 + 0.04L_C - 0.34\Delta + 0.004P_{tl}$	L_C	1.61	0.01	6.97	0.00	0.78	220.86
		Δ	1.32	0.05	−6.74	0.00	—	—
		P_{tl}	1.35	0.00	2.76	0.00	—	—
9	$V_{85} = 64.60 - 0.21\Delta + 0.01P_{tl} + 0.01S_{tl}$	Δ	1.06	0.06	−3.70	0.00	0.62	241.40
		P_{tl}	1.15	0.00	3.81	0.00	—	—
		S_{tl}	1.19	0.00	3.76	0.00	—	—
10	$V_{85} = 68.64 + 0.03L_C - 0.33\Delta + 0.003P_{tl} + 0.004S_{tl}$	L_C	1.89	0.01	5.95	0.00	0.82	215.70
		Δ	1.32	0.05	−7.34	0.00	—	—
		P_{tl}	1.38	0.00	2.57	0.02	—	—
		S_{tl}	1.40	0.00	2.62	0.01	—	—
	Operating speed models on tangents							
11	$V_{85t} = 46.71 + 5.47\ln(P_l)$	P_{tl}	—	0.61	8.91	0.00	0.71	188.03
12	$V_{85t} = 73.41 + 0.001P_{tl} + 0.004S_{tl}$	P_{tl}	1.19	0.00	3.49	0.00	0.47	211.05
	Operating speed reduction models							
13	$\Delta_{85}V = 65.38 - 8.53ln(R)$	R	—	0.81	−10.55	0.00	0.77	191.98
14	$\Delta_{85}V = 5.32 + 8.50ln(D_c)$	D_c	—	0.81	10.51	0.00	0.77	192.18
15	$\Delta_{85}V = 16.34 - 0.04L_C + 0.26\Delta$	Δ	1.06	0.05	4.79	0.00	0.59	214.83
		L_c	1.06	0.01	−5.70	0.00	—	—
	Relation between Δ_{85}V and ΔV$_{85}$							
16	$\Delta_{85} = 5.32 + 0.96\Delta V_{85}$	—	—	0.05	18.90	0.00	0.92	—

Note: EV = explanatory variable; and SE = standard error.

Downloaded from ascelibrary.org by Indian Institute of Technology, Hyderabad on 11/11/22. Copyright ASCE. For personal use only; all rights reserved.

on the horizontal curves. The minimum operating speed was determined for each curve (V_c) from all the sample data, and then the 85th percentile minimum operating speed was calculated for each curve. The preliminary correlation and regression analysis were conducted to examine the relationship between operating speed on the curve and geometric variables. The study developed two lin-log models (Models 1 and 2) and eight multiple linear regression models (Models 3–10) (Table 4). The developed models and their statistical summary are presented in Table 4. The explanatory variables such as curve radius, degree of curve, curve length, and preceding tangent length showed a correlation among themselves, inferring the possibility of multicollinearity. The variance inflation factor (VIF) is used as an indicator of multicollinearity among independent variables and to know the effect of multicollinearity on the model outcomes (Kock and Lynn 2012; Hair et al. 1995; Kabacoff 2011; Ringle et al. 2015; Gujarati 2009). As a common rule of thumb, $\sqrt{\text{vif}} > 2$ indicates that multicollinearity among the independent variables affects the performance of models (Kabacoff 2011). In the present manuscript, the values of VIF were found to be less than the prescribed threshold limits indicating that the performance of the models is not affected due to multicollinearity. The Akaike information criteria (AIC) was used to compare the developed models and choose a suitable model. Of all the developed models, Model 6 resulted in the lowest AIC value. Hence, the study proposed Model 6 as an operating speed model which is a function of curve radius, curve length, and degree of curvature.

The resulting coefficient of determination (R^2) of the proposed model was found to be 0.90 indicating the model explains 90% of the variability of the response data. Also, the significance of explanatory variables, radius, length of curve, and degree of curve was checked at 95% confidence interval ($P < 0.05$). All the variables and their coefficients were found statistically significant at 95% confidence interval. The validation of linear model assumptions was performed for the proposed OLS regression model. From Table 5, p-value $= 0.29$ indicates that the data satisfied the assumptions that follow the OLS regression model. The assumptions are violated if the p-value <0.05 (Peña and Slate 2006). The curve length and degree of curve showed a negative correlation, whereas the curve radius resulted in a positive correlation. Therefore, as the radius of the curve increases, the curve becomes smoother and flatter, allowing the driver to attain higher speeds. Also, with an increase in the curve length and degree of curve, the driver feels that the curve gets sharper resulting in the decrease of the operating speed on the curve.

Operating Speed Model on Tangent

Although several models are available for speed on horizontal curves, predicting operating speed on the tangent segment is

J. Transp. Eng., Part A: Systems, 2020, 146(11): 04020124

Table 5. Global test of linear model assumptions

Measures	Operating speed on curve		Operating speed on tangent		Speed reduction from tangent-to-curve		Decision
	Value	p-value	Value	p-value	Value	p-value	
Global stat	3.43	0.49	1.49	0.83	5.04	0.29	Assumption acceptable
Skewness	0.87	0.35	0.10	0.76	0.56	0.46	Assumption acceptable
Kurtosis	0.05	0.82	0.24	0.63	1.22	0.27	Assumption acceptable
Link function	0.70	0.40	0.01	0.94	1.31	0.25	Assumption acceptable
Heteroscedasticity	1.81	0.18	1.15	0.28	1.96	0.16	Assumption acceptable

Downloaded from ascelibrary.org by Indian Institute of Technology, Hyderabad on 11/11/22. Copyright ASCE. For personal use only; all rights reserved.

considered to be complex (Jacob and Anjaneyulu 2013). The attainment of the free-flow speed on the tangent depends on the available length of the tangent. The tangent speed models were developed considering both dependent and independent tangent lengths. Operating speed on the tangents was used for developing the models. The study developed two models, Models 11 and 12 (Table 4), and the statistically best fit transformed lin-log Model 11 was proposed based on the results of correlation, regression, VIF, and AIC. The resulting coefficient of determination (R^2) for the proposed model was found to be 0.71, and the coefficient of the independent variable was found to be statistically significant at 95% confidence interval ($P < 0.05$). The proposed model met all the statistical assumptions related to the OLS regression model ($p\text{-}value = 0.83$), (refer to Table 5). The operating speed on the tangent and preceding tangent length showed a strong positive correlation. From Fig. 2 it is observed that, operating speed on a tangent (V_{85t}) increases considerably until 250 m, i.e., drivers were found to complete most of their initial acceleration within the first 250 m of the tangent length. Beyond 250 m, V_{85t} was found to increase gradually until drivers reached the desired speed.

Relation between ΔV_{85} and $\Delta_{85}V$

The most commonly used approach to determine the design consistency is based on the calculation of speed difference between successive geometric elements. The maximum and minimum value of the operating speeds on the tangent and curve were calculated for each tangent-to-curve transition and to all the trips. The 85th percentile speed value was determined for tangent and curve for all the tangent-to-curve transitions. The differential of the 85th percentile value for each tangent-to-curve transition was calculated using Eq. (1)

$$\Delta V_{85} = V_{85t} - V_{85} \quad (1)$$

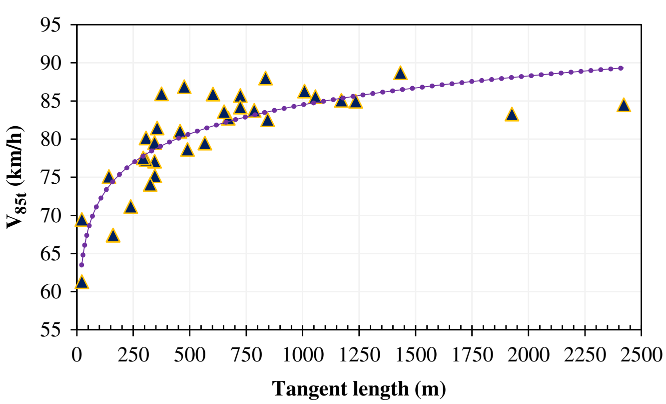

Fig. 2. 85th percentile operating speed prediction model on tangents.

The differential of the 85th percentile speed (ΔV_{85}) may not represent the actual speed reduction because speed distributions at two locations, i.e., on the tangent and curve, are different (Hirsh 1987). Besides, every driver reacts differently to the horizontal curve based on their desirable tangent speed and actual side friction factor (Misaghi and Hassan 2005). Thus, the driver corresponding to the 85th percentile speed on the tangent may not remain the same for the 85th percentile speed on the curve. Hence, Hirsh (1987) suggested from the theoretical point of view to determine the 85th percentile differential for the individual driver to find the actual speed reduction. Thus, in the present study, the value of the 85th percentile speed differential ($\Delta_{85}V$) was calculated for individual vehicles using Eq. (2)

$$\Delta_{85}V = (V_t - V_c)_{85} \quad (2)$$

A relationship between $\Delta_{85}V$ and ΔV_{85} was established to understand their significance. The statistical summary of the developed relation is shown in Table 4 (Model 16). The relationship between $\Delta_{85}V$ and ΔV_{85} was found to be a straight line parallel to the line representing $\Delta_{85}V = \Delta V_{85}$ (Fig. 3) with $\Delta_{85}V$ higher than ΔV_{85} by 5.32 km/h. This value is in good agreement with the values reported in the previous literature for passenger cars (Castro et al. 2011; Pérez-Zuriaga et al. 2013; Montella et al. 2013). The differential of 85th percentile speed (ΔV_{85}) obtained by simple subtraction of the 85th percentile speed value on tangent and curve underestimated the actual speed reduction because the speed distributions at two locations are different. Thus, the 85th percentile driver on tangent may not remain the same for the 85th percentile driver on the curve. Hence, $\Delta_{85}V$ was introduced, which determines the actual speed reduction corresponding to the individual driver. The resulting R^2 of the proposed model was found to be 0.92,

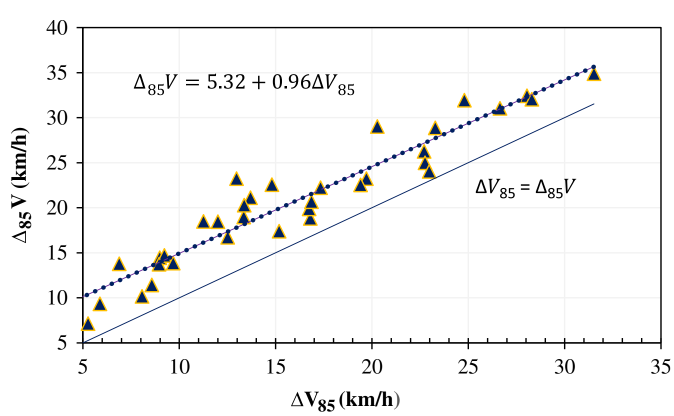

Fig. 3. Relationship between 85th percentile speed differential ($\Delta_{85}V$) and differential of the 85th percentile ($\Delta_{85}V$).

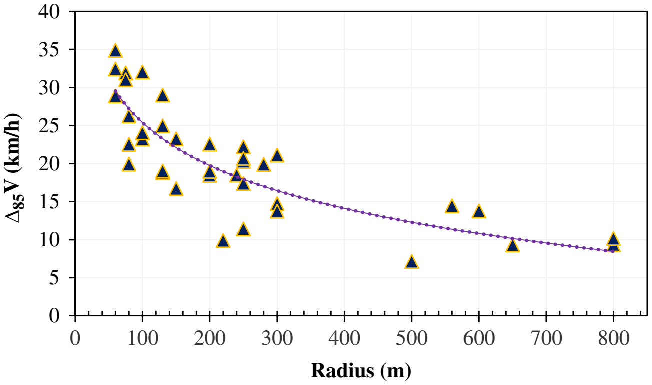

Fig. 4. 85th percentile operating speed differential model.

and the coefficient of the independent variable was significantly different from zero at 95% confidence interval ($P < 0.05$).

Speed Reduction Model

Based on the previous discussion, the 85th percentile speed differential ($\Delta_{85}V$) determined the actual speed reduction between successive geometric elements. The correlation for operating speed reduction from tangent-to-curve and various other geometric elements is presented in Table 3. The 85th percentile speed differential ($\Delta_{85}V$) showed a strong negative correlation with the curve radius. Regression analysis was performed, and two lin-log models, Models 13 and 14 and one multiple linear regression model, Model 15, were developed. The developed models and their statistical summary is presented in Table 4. From Table 4, it is clear that Model 13 resulted in the lowest AIC value and therefore was proposed for predicting the operating speed reduction with radius (R) as an explanatory variable. The resulting R^2 for the proposed model was 0.77, and the coefficient of the independent variable was significantly different from zero at the 95% confidence interval ($P < 0.05$). The proposed model satisfied all the OLS regression model assumptions ($p\text{-}value = 0.29$), as shown in Table 5. The negative and significant coefficient of radius indicates that as the radius of curve decreases, the speed reduction from tangent-to-curve increases. The curve gets sharper with a decrease in the radius leading to the attainment of lower speeds on the curve. Fig. 4, depicts the change in $\Delta_{85}V$ with respect to the radius. It is observed that the decrease in $\Delta_{85}V$ is significant until 300 m, and thereafter it decreases gradually as the radius increases.

Model Validation and Comparison

Preliminary validation was conducted for measuring the degree of correspondence of the predicted operating speed with the field data. The models were validated with the speed data collected at similar sites, which fulfilled the criteria in the model development. Also, a

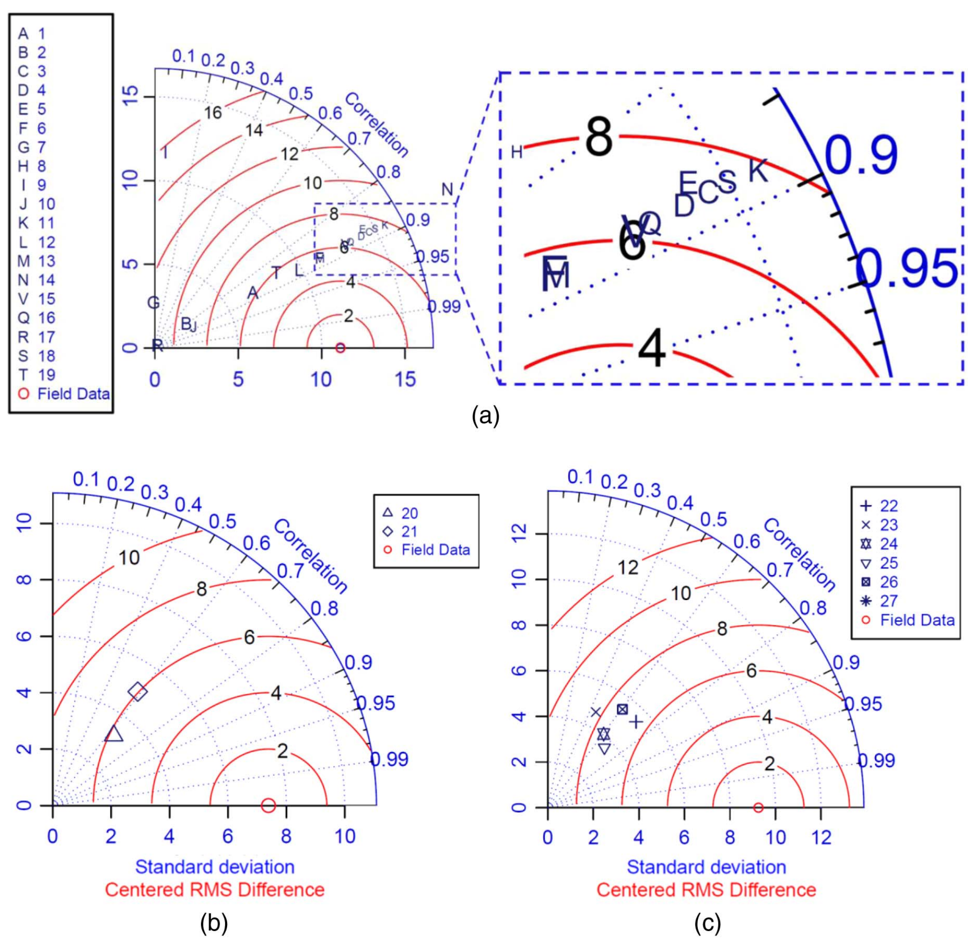

Fig. 5. Taylor diagram showing statistical comparison with observations of 27 models estimates of the: (a) speed on curve; (b) speed on tangent; and (c) speed reduction from tangent-to-curve.

J. Transp. Eng., Part A: Systems, 2020, 146(11): 04020124

Downloaded from ascelibrary.org by Indian Institute of Technology, Hyderabad on 11/11/22. Copyright ASCE. For personal use only; all rights reserved.

comparative study was made between the existing speed prediction models available in the literature and the proposed models in the present study. Various factors were considered while selecting the models from the literature for comparative analysis; this includes geometric characteristics, data collection methodology, model significance, type of terrain, type of vehicle, and geographical variation. In the present study, the Taylor diagram was used for model validation and comparison. The Taylor diagram depicts a concise statistical summary of how well a pattern (or a set of patterns) matches observations/field data in terms of their correlation, their centered root-mean-square (CRMS) difference, and the standard deviation (Taylor 2005). These statistics provide a quick summary of the degree of pattern/patterns correspondence, allowing one to ascertain how accurately a model counterfeits the ground truth. The simulated patterns that accord well with the field data will lie closest to the point *Field data* marked on the x axis (Fig. 5). The values of MAD (mean absolute deviation) and RMSE (root mean square error) of the models were also calculated for validation [Eqs. (3) and (4)]

$$\text{Mean absolute difference (MAD)} = \frac{\sum_{i=1}^{n} |observed_i - predicted_i|}{n} \tag{3}$$

$$\text{Root mean square error (RMSE)} = \sqrt{\frac{\sum_{i=1}^{n} (observed_i - predicted_i)^2}{n}} \tag{4}$$

where n is the number of observations.

Fig. 5(a) shows a Taylor diagram used to summarize the relative skill with which several speed models simulate the spatial pattern of operating speed on the curve with field data. Statistics of the 27 models (Table 6) were computed, and a letter/symbol is assigned to each of the models contemplated. The location of each letter on the plot determines how fairly the model's simulated pattern replicates the field data. The proposed operating speed model for horizontal curves (Model 1) from the present study was validated and compared with models available in the literature. To illustrate, consider Model 1, its pattern correlation with the field data is 0.87. The red contours represent CRMS as the difference between the simulated pattern (or set of patterns) and observed/field data, which is between 5 and 7 km/h [Fig. 5(a)]. The radial distance from the origin to the simulated paterns represents the standard deviation. In the case of Model 1, the standard deviation is about 7.03 km/h, which is low compared with field data (~11.6 km/h). The relative goodness of the speed models is summarized in Fig. 5(a).'

The simulated patterns of Models 1, 12, and 19 showed strong pattern correlation (~0.8 to 0.9), each with approximately the CRMS error between 5 and 7 km/h. The standard deviation of the simulated patterns is less than the field data (~11.58 km/h) [Fig. 5(a)]. Models 3–6, 8, 11, 13–16, and 18 resulted in strong pattern correlation (~0.8–0.9). However, the CRMS errors (~ > 5 km/h), and standard deviations were greater in comparison with Models 1, 12, and 19. Simulated patterns of Models 2, 10, and 17 showed moderate to strong pattern correlation (~0.6–0.9), and CRMS greater than 8 km/h. Models 2, 10, and 17 showed lower pattern correlation, and higher CRMS error compared with Models 1, 12, and 19. Models 8 and 10 showed very weak pattern correlation (~ < 0.2), CRMS between 11 and 16 km/h.

Table 6. Features of the compared speed and deceleration models

Model No	Authors	Models	MAD	RMSE
		Operating speed models on curves		
1	Proposed model	$V_{85} = 72.10 + 0.02R - 0.01L_C - 1.14D_C$	5.58	6.52
2	Jacob and Anjaneyulu (2013)	$V_{85} = 56.75 - (739.21/R) - 0.034L_c$	12.83	17.85
3	Zuriaga et al. (2010)	$V_{85} = 97.43 - (3310.94/R)$	7.57	12.40
4	Lamm and Choueiri (1987)	$V_{85} = 94.397 - (3189.24/R)$	5.97	10.49
5	Kanellaidis et al. (1990)	$V_{85} = 129.88 - (623.13/\sqrt{R})$	10.92	17.06
6	Krammes et al. (1995)	$V_{85} = 102.44 - (2471.81/R) + 0.021L_C - 0.10\Delta$	12.17	19.00
7	Gibreel et al. (2001)	$V_{85} = 102.2 - 0.11\Delta$	20.84	36.31
8	Castro et al. (2008)	$V_{85} = 120.16 - (5596.72/R)$	13.92	22.50
9	Castro et al. (2011)	$V_{85} = 91.13 + 0.03L_C - 0.48\Delta$	8.75	18.86
10	Morrall and Talarico (1994)	$V_{85} = \exp(4.56 - 0.00586D_C)$	17.37	29.54
11	Islam and Seneviratne (1994)	$V_{85} = 103.30 - 2.41D_C - 0.029D_C^2$	12.83	18.93
12	McFadden and Elefteriadou (2000)	$V_{85} = 103.66 - 1.95D_C$	16.30	24.86
13	Taragin and Leisch (1954)	$V_{85} = 88.87 - (2554.76/R)$	4.75	9.01
14	Glennon et al. (1986)	$V_{85} = 103.96 - (4524.94/R)$	7.50	13.81
15	Voigt (1996)	$V_{85} = 99.61 - (2951.37/R)$	10.56	16.19
16	Passetti and Fambro (1999)	$V_{85} = 103.90 - (3020.50/R)$	13.24	19.79
17	Misaghi and Hassan (2005)	$V_{85} = 94.30 + (8.67E - 6)(R^2)$	19.24	33.54
18	Ottesen and Krammes (1994)	$V_{85} = 103.70 - (3403/R)$	11.53	17.39
19	Ottesen and Krammes (2000)	$V_{85} = 102.44 - 1.57D_C - 0.012L_c - 0.01D_CL_c$	11.20	18.70
		Operating speed models on tangents		
20	Proposed model	$V_{85t} = 46.71 + 5.47\ln(P_{tl})$	4.54	5.85
21	Jacob and Anjaneyulu (2013)	$V_{85t} = 69.00 - (1005.39/R) - 0.065L_c$	27.19	28.07
		Speed reduction models from tangent-to-curve		
22	Proposed model	$\Delta_{85}V = 65.38 - 8.53ln(R)$	5.98	7.01
23	Jacob and Anjaneyulu (2013)	$\Delta_{85}V = -26.44 - 0.0066R - 0.018L_C + 0.71V_t$	7.31	8.43
24	Pérez-Zuriaga et al. (2013)	$\Delta_{85}V = 9.051 + (1527.33/R)$	7.24	8.75
25	Abdelwahab et al. (1998)	$\Delta V_{85} = 0.9433D_C + 0.0847\Delta$	12.20	14.20
26	Al-Masaeid et al. (1995)	$\Delta_{85}V = 3.64 + 1.78D_C$	8.29	10.40
27	Choudhari and Maji (2019)	$\Delta_{85}V = 2.87 + (1388.42/R) + 0.05P_{TL}$	32.02	40.00

Downloaded from ascelibrary.org by Indian Institute of Technology, Hyderabad on 11/11/22. Copyright ASCE. For personal use only; all rights reserved.

Downloaded from ascelibrary.org by Indian Institute of Technology, Hyderabad on 11/11/22. Copyright ASCE. For personal use only; all rights reserved.

Models 1, 12, and 19 were found to be approximately at the same distance from field data marked on the X axis. Thus, the simulated patterns of the Model 1, 12, and 19 showed a high degree of correspondence with field data and were found to be good predictors of operating speed on horizontal curves.

Similarly, the Taylor diagram was used to validate the operating speed models on a tangent and speed reduction from tangent-to-curve. In the present study, Model 20 was developed to predict the operating speed on a tangent (Table 6). Model 20 showed the pattern correlation coefficient value of 0.64 and centered RMS approximately equal to 5.86 km/h. The standard deviation of Model 20 was lower than the standard deviation of the field data (~7.84 km/h) [Fig. 5(b)]. Also, the model represented lower MAD and RMSE values (Table 6). The simulated pattern of Model 21 given by Jacob and Anjaneyulu (2013) showed a moderate correlation (~0.58), high centered RMS (~ > 6.05 km/h) in comparison with Model 21. Hence, Model 20 is proposed as it showed low errors and variations in comparison to Model 21.

In the case of speed reduction models, Model 22 (Table 6) was proposed. Model 22 was found to have a strong pattern correlation (~0.72), and CRMS value of 6.38 km/h. Also, the standard deviation was found to be 5.61 km/h, which was lower than that of field data (~9.63 km/h) [Fig. 5(c)]. Whereas the simulated patterns of Models 23, 24, 25, and 26 showed moderate to strong correlation and high centered RMS [Fig. 5(c)] in comparison with Model 22. Also, the models represented the higher MAD, and RMSE in comparison with Model 22 (Table 6). Model 27 is not represented in Taylor's diagram because it showed a very weak pattern correlation (~ < 0.02) and high errors and deviations (Table 6). The simulated spatial pattern of proposed Model 22 showed a high degree of correspondence with the field data and was found to be a predictor of speed reduction.

Conclusions

The paper documents an experimental examination of the operating speed variation of the drivers on horizontal curves, tangents, and tangent-to-curve transitions using continuous speed profiles for two-lane rural highways in India. The data collection methodology enabled us to accurately determine the maximum and minimum speed positions on the successive geometric elements and to develop reliable operating speed prediction models. Preliminary correlation analysis and regression were used to develop the models as a function of various geometric variables. In total, 15 models were developed and analyzed, of which four models were proposed in this study. A relation between $\Delta_{85}V$ and ΔV_{85} from tangent-to-curve was also established. Taylor's diagram was used to compare the proposed models with the existing models from the literature with similar explanatory variables for different countries. Besides, the models were validated with the field data collected from similar geometric features as used in the development of the regression models. The following conclusions were drawn from the study:

1. The differential of the 85th percentile speed (ΔV_{85}) was found to underestimate the actual speed reduction calculated using 85th percentile speed differential ($\Delta_{85}V$) by 5.32 km/h. The results were in good agreement with the theoretical argument by Hirsh (1987) and findings of Zuriaga et al. (2010), and McFadden and Elefteriadou (2000).
2. Curve radius, deflection angle, degree of curve, and curve length were found to significantly affect the operating speed on the horizontal curves.
3. The proposed operating speed models on curve, tangent, and tangent-to-curve showed moderate to strong correlation, low errors, and variations referencing field data and other available models in the literature.
4. Finally, the study concludes that the models developed using continuous speed profile data are more promising in predicting operating speed compared with the models developed using spot speed data. This indicates that data collection methodology using instrumented vehicle acts as a promising tool in inspecting the driver behavior and developing models that accurately estimate the speed parameters.

Future research may consider developing operating speed models for roads with gradient and different vehicle types. Also, the robustness of the developed models can be checked using the data from the long-term naturalistic studies. Though collecting continuous speed profile data for different vehicle types using long-term naturalistic studies is a challenging and exhaustive task; the research would add great value to the existing literature because it will lead to more reliable and robust models.

Data Availability Statement

Some or all data, models, or code that support the findings of this study are available from the corresponding author upon reasonable request.

References

AASHTO. 2011. *A policy on geometric design of highways and streets*. Washington, DC: AASHTO.

Abdelwahab, W. M., M. T. Aboul-Ela, and J. F. Morrall. 1998. "Geometric design consistency based on speed change on horizontal curves." *Road Transp. Res.* 127 (1): 13–23.

Ahmed, I. 2013. "Road infrastructure and road safety." *Transp. Commun. Bull. Asia Pac.* 83 (1): 19–25.

Albin, R., et al. 2016. *Low-cost treatments for horizontal curve safety 2016*. Rep. No. FHWA-SA-15-084. Washington, DC: Federal Highway Administration.

Al-Masaeid, H. R., M. Hamed, M. Aboul-Ela, and A. G. Ghannam. 1995. "Consistency of horizontal alignment for different vehicle classes." *Transp. Res. Rec.* 1500 (Dec): 178–783.

Andueza, P. J. 2000. "Mathematical models of vehicular speed on mountain roads." *Transp. Res. Rec.* 1701: 104–110. https://doi.org/10.3141/1701-13.

Calvi, A., and F. Bella. 2014. "Modeling speed differential parameters in day and night environments using driving simulator." *Procedia Eng.* 84: 648–661. https://doi.org/10.1016/j.proeng.2014.10.482.

Castro, M., L. Iglesias, R. Rodriguez-Solano, and J. A. Sanchez. 2008. "Highway safety analysis using geographic information systems." In Vol. 161 of *Proc., Institution of Civil Engineers—Transport*, 91–97. London: Thomas Telford.

Castro, M., J. F. Sánchez, J. A. Sánchez, and L. Iglesias. 2011. "Operating speed and speed differential for highway design consistency." *J. Transp. Eng.* 137 (11): 837–840. https://doi.org/10.1061/(ASCE)TE.1943-5436.0000309.

Choudhari, T., and A. Maji. 2019. "Effect of horizontal curve geometry on the maximum speed reduction: A driving simulator-based study." *Transp. Developing Economies* 5 (2): 14. https://doi.org/10.1007/s40890-019-0082-8.

Dhahir, B., and Y. Hassan. 2018. "Studying driving behaviour on horizontal curves using naturalistic driving study data." *Transp. Res. Rec.* 2672 (17): 83–95. https://doi.org/10.1177/0361198118784384.

Dhahir, B., and Y. Hassan. 2019. "Using horizontal curve speed reduction extracted from the naturalistic driving study to predict curve collision frequency." *Accid. Anal. Prev.* 123 (Feb): 190–199. https://doi.org/10.1016/j.aap.2018.11.020.

Elliott, G., A. Gargano, and A. Timmermann. 2013. "Complete subset regressions." *J. Econom.* 177 (2): 357–373. https://doi.org/10.1016/j.jeconom.2013.04.017.

Fitzpatrick, K., et al. 2000. *Speed prediction for two-lane rural highways*. Rep. No. FHWA-RD-99-171. Washington, DC: Federal Highway Administration.

Fitzpatrick, K., and J. M. Collins. 2000. "Speed-profile model for two-lane rural highways." *Transp. Res. Rec.* 1737 (1): 42–49. https://doi.org/10.3141/1737-06.

García, A., D. Llopis-Castelló, F. J. Camacho-Torregrosa, and A. M. Pérez-Zuriaga. 2013. "New consistency index based on inertial operating speed." *Transp. Res. Rec.* 2391 (1): 105–112. https://doi.org/10.3141/2391-10.

Gibreel, G. M., S. M. Easa, and I. A. El-Dimeery. 2001. "Prediction of operating speed on three-dimensional highway alignments." *J. Transp. Eng.* 127 (1): 21–30. https://doi.org/10.1061/(ASCE)0733-947X(2001)127:1(21).

Gibreel, G. M., S. M. Easa, Y. Hassan, and I. A. El-Dimeery. 1999. "State of the art of highway geometric design consistency." *J. Transp. Eng.* 125 (4): 305–313. https://doi.org/10.1061/(ASCE)0733-947X(1999)125:4(305).

Glennon, J. C., T. R. Neuman, and J. E. Leisch. 1986. *Safety and operational considerations for design of rural highway curves*. Rep. No. FHWA/RD-86/035. Mclean, VA: Federal Highway Administration.

Gujarati, D. N. 2009. *Basic econometrics*. New York: McGraw-Hill.

Hair, J. F., R. E. Anderson, R. L. Tatham, and W. C. Black. 1995. *Multivariate data analysis*. Englewood Cliffs, NJ: Prentice-Hall.

Hassan, Y. 2004. "Highway design consistency: Refining the state of knowledge and practice." *Transp. Res. Rec.* 1881 (1): 63–71. https://doi.org/10.3141/1881-08.

Hirsh, M. 1987. "Probabilistic approach to consistency of highway alignment." *J. Transp. Eng.* 113 (3): 268–276. https://doi.org/10.1061/(ASCE)0733-947X(1987)113:3(268).

Islam, M., and P. Seneviratne. 1994. "Evaluation of design consistency of two-lane rural highways." *ITE J.* 64 (2): 28–31.

Jacob, A., and M. V. L. R. Anjaneyulu. 2013. "Operating speed of different classes of vehicles at horizontal curves on two-lane rural highways." *J. Transp. Eng.* 139 (3): 287–294. https://doi.org/10.1061/(ASCE)TE.1943-5436.0000503.

Kabacoff, R. I. 2011. *R in action: Data analysis and graphics with R*. 2nd ed. Shelter Island, NY: Manning Publications.

Kanellaidis, G., J. Golias, and S. Efstathiadis. 1990. "Drivers' speed behaviour on rural road curves." *Traffic Eng. Control* 31 (7–8): 414–415.

Kock, N., and G. Lynn. 2012. "Lateral collinearity and misleading results in variance-based SEM: An illustration and recommendations." *J. Assoc. Inf. Syst.* 13 (7): 546–580. https://doi.org/10.17705/1jais.00302.

Krammes, R. A. 1997. "Interactive highway safety design model: Design consistency module." *Public Roads* 61 (2): 47–51.

Krammes, R. A., K. S. Rao, and H. Oh. 1995. "Highway geometric design consistency evaluation software." *Transp. Res. Rec.* 1500 (Dec): 19–24.

Krehbiel, T. C. 2004. "Correlation coefficient rule of thumb." *Decis. Sci. J. Innovative Educ.* 2 (1): 97–100. https://doi.org/10.1111/j.0011-7315.2004.00025.x.

Lamm, R., and E. M. Choueiri. 1987. "Recommendations for evaluating horizontal design consistency based on investigations in the state of New York." *Transp. Res. Rec.* 1122 (May): 68–78.

Lamm, R., E. M. Choueiri, J. C. Hayward, and A. Paluri. 1988. "Possible design procedure to promote design consistency in highway geometric design on two-lane rural roads." *Transp. Res. Rec.* 1195 (Nov): 111–122.

Lamm, R., B. Psarianos, and T. Mailaender. 1999. *Highway design and traffic safety engineering handbook*. New York: McGraw-Hill.

Maji, A., G. Sil, and A. Tyagi. 2018. "85th and 98th percentile speed prediction models of car, light, and heavy commercial vehicles for four-lane divided rural highways." *J. Transp. Eng., Part A: Systems* 144 (5): 04018009. https://doi.org/10.1061/JTEPBS.0000136.

McFadden, J., and L. Elefteriadou. 2000. "Evaluating horizontal alignment design consistency of two-lane rural highways: Development of new procedure." *Transp. Res. Rec.* 1737 (1): 9–17. https://doi.org/10.3141/1737-02.

Misaghi, P., and Y. Hassan. 2005. "Modeling operating speed and speed differential on two-lane rural roads." *J. Transp. Eng.* 131 (6): 408–418. https://doi.org/10.1061/(ASCE)0733-947X(2005)131:6(408).

Montella, A., F. Galante, L. Liani Imbriani, F. Mauriello, M. Pernetti, and V. Ranieri. 2013. "Evaluation of driving behaviour on horizontal curves of two-lane rural highways: Driving simulator experiment." In *Proc., 4th Road Safety and Simulation Int. Conf.* Washington, DC: Federal Highway Administration.

Montella, A., L. Pariota, F. Galante, L. L. Imbriani, and F. Mauriello. 2014. "Prediction of drivers' speed behavior on rural motorways based on an instrumented vehicle study." *Transp. Res. Rec.* 2434 (1): 52–62. https://doi.org/10.3141/2434-07.

Morrall, J. F., and R. J. Talarico. 1994. "Side friction demanded and margins of safety on horizontal curves." *Transp. Res. Rec.* 1435 (Oct): 145–152.

MORTH (Ministry of Road Transport and Highways). 2018. *Road accidents in India 2018*. New Delhi, India: MORTH.

Ottesen, J., and R. Krammes. 2000. "Speed-profile model for a design-consistency evaluation procedure in the United States." *Transp. Res. Rec.* 1701 (1): 76–85. https://doi.org/10.3141/1701-10.

Ottesen, J. L., and R. A. Krammes. 1994. "Speed profile model for a US operating speed-based consistency evaluation procedure." In *Proc., 73rd Annual Meeting of Transportation Research Board*. Washington, DC: Transportation Research Board.

Passetti, K. A., and D. B. Fambro. 1999. "Operating speeds on curves with and without spiral transitions." *Transp. Res. Rec.* 1658 (1): 9–16. https://doi.org/10.3141/1658-02.

Peña, E. A., and E. H. Slate. 2006. "Global validation of linear model assumptions." *J. Am. Stat. Assoc.* 101 (473): 341–354. https://doi.org/10.1198/016214505000000637.

Pérez-Zuriaga, A. M., F. J. Camacho-Torregrosa, and A. García. 2013. "Tangent-to-curve transition on two-lane rural roads based on continuous speed profiles." *J. Transp. Eng.* 139 (11): 1048–1057. https://doi.org/10.1061/(ASCE)TE.1943-5436.0000583.

Ringle, C. M., S. Wende, and J. M. Becker. 2015. *SmartPLS 3*. Bönningstedt, Germany: SmartPLS.

Sil, G., S. Nama, A. Maji, and A. K. Maurya. 2019. "Modeling 85th percentile speed using spatially evaluated free-flow vehicles for consistency-based geometric design." *J. Transp. Eng., Part A: Systems* 146 (2): 04019060. https://doi.org/10.1061/JTEPBS.0000286.

Taragin, A., and L. E. Leisch. 1954. "Driver performance on horizontal curves." In Vol. 33 of *Proc., 33rd Annual Meeting of the Highway Research Board*. Washington, DC: Highway Research Board.

Taylor, K. E. 2005. "Summarizing multiple aspects of model performance in a single diagram." *J. Geophy. Res.* 106 (D7): 7183–7192.

Voigt, A. 1996. *An evaluation of alternative horizontal curve design approaches for rural two-lane highways*. Rep. No. TTI-04690-3. College Station, TX: Texas Transportation Institute.

Wang, K., and Z. Chen. 2016. "Stepwise regression and all possible subsets regression in education." *Electron. Int. J. Educ. Arts Sci.* 2 (1): 60–81.

Zuriaga, A. M. P., A. G. García, F. J. C. Torregrosa, and P. D'Attoma. 2010. "Modeling operating speed and deceleration on two-lane rural roads with global positioning system data." *Transp. Res. Rec.* 2171 (1): 11–20. https://doi.org/10.3141/2171-02.

Downloaded from ascelibrary.org by Indian Institute of Technology, Hyderabad on 11/11/22. Copyright ASCE. For personal use only; all rights reserved.

J. Transp. Eng., Part A: Systems, 2020, 146(11): 04020124